[CANCER RESEARCH 61, 6428–6436, September 1, 2001]

A Hepatocellular Carcinoma-specific Adenovirus Variant, CV890, Eliminates Distant Human Liver Tumors in Combination with Doxorubicin

Yuanhao Li, De-Chao Yu, Yu Chen, Pinky Amin, Hong Zhang, Natalie Nguyen, and Daniel R. Henderson[1]

Calydon, Inc., Sunnyvale, California 94089

ABSTRACT

Hepatocellular carcinoma (HCC) is the third leading cause of cancer death in the world. Tumor resection remains the only curative treatment but is often not possible because of advanced stage and frequently unsuccessful because of intrahepatic or distant tumor recurrence. α-Fetoprotein (AFP), a tumor marker currently used for the diagnosis and management of HCC, is an oncofetal protein expressed in a majority of HCCs but rarely in normal hepatocytes. Because AFP gene expression is tightly regulated at the level of transcription, AFP transcriptional regulatory elements (TRE) are excellent candidates for generating HCC-specific oncolytic adenoviruses. We devised a new strategy for the AFP TRE to control an artificial E1A-IRES-E1B bicistronic cassette in an adenovirus 5 vector (Ad5) and constructed an HCC-specific oncolytic virus, CV890. *In vitro*, CV890 expression of the *E1A* and *E1B* genes, virus replication, and cytopathic effects were examined by Northern blot, Western blot, virus yield assay, and 3-(4,5-dimethylthiazol-2-yl)-2,5-diphenyltetrazolium bromide assay in AFP-producing cell lines (HepG2, Huh7, Hep3B, PLC/PRF/5, and SNU449), non-AFP-producing cell lines (Sk-Hep-1, Chang liver cell, LNCaP, HBL-100, PA-1, UM-UC-3, SW 780, Colo 201, and U118 MG), and non-AFP-producing human primary cells (lung fibroblast, bladder smooth muscle, and mammary epithelial). CV890 efficiently replicates in and destroys AFP-producing HCC cells as well as wild-type Ad5, but replication is highly attenuated in non-AFP-producing HCC cells or non-HCC cells. CV890 produced 5,000–100,000-fold less virus than wild-type Ad5 in non-AFP-producing cells. CV890 was attenuated 100-fold more than CV732, a virus containing the AFP TRE driving the *E1A* gene alone, in non-AFP-producing cells. These studies demonstrated that expression of both *E1A* and *E1B* genes under the control of a bicistronic AFP-E1A-IRES-E1B cassette yielded improvements in virus specificity equivalent to driving the *E1A* and *E1B* genes with two independent TREs yet requires only one TRE thereby conserving genomic space within the virus. Significantly, CV890 produced nearly the same yield of virus in cells that produced AFP over a 75-fold range, from a low of 60 ng AFP/10^6 cells/10 days to as high as 4585 ng AFP/10^6 cells/10 days. *In vivo*, antitumor efficacy of CV890 was examined in BALB/c-*nu/nu* mice containing large s.c. HepG2 or Hep3B tumor xenografts. Tumor volume of distant xenografts dropped below baseline 4 weeks after a single i.v. injection. Combination of CV890 with doxorubicin demonstrated synergistic antitumor efficacy, yielding complete elimination of distant Hep3B tumors 4 weeks after a single i.v. administration of both compounds. Our results support the clinical development of CV890 as an antineoplastic agent for the treatment of localized or metastatic HCC.

INTRODUCTION

HCC[2] is the third leading cause of cancer death in the world (1, 2). Tumor resection is the only curative treatment but is often unsuccessful because patients die of intrahepatic or distant tumor recurrence (3–6). HCC is refractory to chemotherapy because of tumor heterogeneity and the development of multidrug resistance phenotypes (7). We are developing novel therapeutics by modifying adenovirus to control essential viral genes with tumor-specific TREs, so as to specifically replicate in and destroy certain types of carcinoma cells (8–10). AFP is a protein expressed by the fetus during gestation but not expressed after birth. In the majority of HCC, AFP is re-expressed, whereas in normal hepatocytes or in regenerating cirrhotic liver, AFP is rarely expressed or expressed to a significantly lesser degree (11). Serum AFP levels are widely used in the diagnosis and management of HCC (12). AFP concentration tends to increase with disease progression, and high levels of AFP are found in patients with advanced HCC. Whereas the role of AFP in HCC development is unclear, the elements that regulate its transcription have been studied extensively. Previous work has identified HCC-specific enhancer domains, silencer elements, and a glucocorticoid responsive element that tightly regulate AFP expression at the level of transcription (13, 14). Thus, the AFP TRE is an excellent candidate for applying our new gene therapy strategies to HCC.

To target the oncolytic adenoviruses to specific tumors, we and others have used tumor- or tissue-specific promoters to restrict the virus replication to target tumor cells (8–10, 15). In the first 2.5 h after adenovirus infection, the *E1A* gene is the only viral gene transcribed. The E1A proteins transactivate both viral and cellular genes critical for productive viral infection including E1B, E2, and E4 (16). Adenovirus *E1B* genes are also expressed relatively early in viral infection. The E1B proteins inhibit E1A-induced p53-dependent apoptosis, aid in the cytoplasmic accumulation of late viral mRNA, and promote shutoff of host cell protein synthesis (17). Previous studies have shown that E1A expression controlled by a specific TRE can initiate the selective replication of the recombinant adenoviruses in target cells while restricting replication in nontarget cells (8–10, 15). However, the leakiness of foreign TREs in E1A control yielding low levels of E1A may result in loss of specificity (18, 19). To control the viral replication more stringently, we explored previously use of a second transcriptional control to control E1B (9, 10). We demonstrated that separated TRE control of both the *E1A* and *E1B* genes significantly improved the specificity and the *in vitro* therapeutic index of CV764 and CV787, two prostate cancer-specific adenovirus variants (9, 10). However, the two TRE sequences must contain ≥20% heterologous sequences to prevent homologous recombination that deletes the intervening E1A sequence during replication (9, 10). Primary liver cancer currently has only a single well-characterized TRE that demonstrates tumor cell specificity. Therefore, we devised an alternate strategy to retain the high level of specificity for target cells obtained by controlling expression of the *E1A* and *E1B* genes with a single TRE. In this communication, we demonstrated that an AFP-E1A-IRES-E1B bicistronic expression cassette fulfilled the necessary requirements and created an AFP-producing hepatoma-specific adenovirus variant, CV890, for additional clinical development.

Of concern clinically is whether oncolytic viruses replicate in and destroy tumor cells expressing varying levels and, in particular, low levels of the tumor marker. This question is difficult to ask of the prostate-specific viruses CV706 and CV787 in the prostate cancer

Received 2/28/01; accepted 6/21/01.

The costs of publication of this article were defrayed in part by the payment of page charges. This article must therefore be hereby marked *advertisement* in accordance with 18 U.S.C. Section 1734 solely to indicate this fact.

[1] To whom requests for reprints should be addressed, at Calydon, Inc., 1324 Chesapeake Terrace, Sunnyvale, CA 94089. Phone: (408) 734-0733; Fax: (408) 734-2808; E-mail: dhenderson@calydon.com.

[2] The abbreviations used are: HCC, hepatocellular carcinoma; ARCA, attenuated replication competent adenovirus; ECL, enhanced chemiluminescence; EMCV, encephelomycarditis virus; nt, nucleotide; Ad5, adenovirus type 5; E3, E3 region of Ad5; wt, wild-type; TRE, transcription response element; AFP, α-fetoprotein; IRES, internal ribosome entry site; PSA, prostate-specific antigen; MTT, 3-(4,5-dimethylthiazol-2-yl)-2,5-diphenyltetrazolium bromide; MOI, multiplicity of infection(s); pfu, plaque-forming units; CV, Calydon virus.

system because of the lack of different prostate cancer cells lines expressing varying levels of PSA. This is not the case in the liver cancer system, because many cell lines expressing AFP are available. We show that CV890 replication in AFP^+ cells is nearly independent of AFP production levels between 60 ng and 4500 ng AFP/10^6 cells/10 days, a 75-fold range. Also clinically, once tumor specificity is attained, the focus shifts to efficacy. With CV890 we extend our previous observations that reintroduction of the adenovirus E3 region into these constructs and synergy with chemotherapy both independently increase the efficacy of oncolytic adenoviruses (9, 20).

MATERIALS AND METHODS

Cells. HCC cell lines HepG2, Hep3B, PLC/PRF/5, SNU449, and Sk-Hep-1, Chang liver cell (human normal liver cells), as well as tumor cell lines PA-1 (ovarian carcinoma), UM-UC-3 (bladder carcinoma), SW 780 (bladder carcinoma), HBL100 (breast epithelia), Colo 201 (Colon adenocarcinoma), U118 MG (glioblastoma), and LNCaP (prostate carcinoma) were obtained from the American Type Culture Collection. HuH-7 (liver carcinoma) was a generous gift of Dr. Patricia Marion (Stanford University, Stanford, CA). Human embryonic kidney cells containing the E1 region of adenovirus (293 cells) were purchased from Microbix, Inc. (Toronto, Canada). The primary cells (normal human bladder smooth muscle cells, normal human lung fibroblast cells, and normal human mammary epithelial cells) were purchased from Clonetics (San Diego, CA). All of the tumor cell lines were maintained in RPMI 1640 (BioWhittaker, Inc.) supplemented with 10% fetal bovine serum (Irvine Scientific), 100 units/ml penicillin, and 100 μg/ml streptomycin. Primary cells were maintained in accordance with vendor instructions (Clonetics). Cells were tested for the expression of AFP by immunoassay (Genzyme Diagnostics, San Carlos, CA).

Plasmid Construction. A composite AFP TRE that includes an AFP enhancer and promoter element was assembled by overlap PCR and cloned into adenovirus. The enhancer element (−3756 bp-−3167 bp) was amplified from human genomic DNA (Clontech, Palo Alto, California) with primers 39.055B (5′-gtgaccggtgcattgctgtgaactcacgt) and 39.055D (5′-ataagtggcctggataaagctgatgca). The promoter (−123 bp-+14 bp) was amplified with primers 39.055J (5′-gtcaccggtctttgttattggcagaatt) and 39.055M (5′-atccaggccacttatgagctctgtgtggaa). The two products were annealed and used as the template for PCR with primers 39.055B and 39.055J. A 0.8 kb *Pin*AI (isoschizomer of *Age*I) fragment from this overlap product was used as the AFP TRE.

To control both the Ad5 E1A and E1B expression from a single TRE, an IRES from EMCV was introduced into the junction of these two genes. A 0.5 kb EMCV IRES fragment was placed into the E1A-E1B modified intergenic region to form the bicistronic E1A-IRES-E1B cassette. The final plasmid, CP686, was generated by placing a 0.8 kb *Pin*AI fragment that contains the AFP TRE in front of the bicistronic E1A-IRES-E1B cassette (detail structure will be reported elsewhere). Another plasmid, CP219, containing a single AFP-control E1A expression was derived from CP124 (10) by placing the *Pin*AI fragment containing the AFP TRE to the *Pin*AI site in front of the E1A coding region. All of the DNA manipulations were performed according to established protocols (9, 10).

Virus Construction. CV890 was constructed by cotransfection of the 293 low-passage cells with CP686 and pBHGE3 (9, 10). Briefly, CP686 and pBHGE3 DNA were cut by appropriate endonuclease digestion and transfected using Lipofectin (Life Technologies, Inc., Grand Island, New York) in a 4:1 molar ratio of lipid to DNA. Transfections were incubated for 7–14 days, harvested, freeze-thawed, and plaqued on the 293 cells. Potential recombinant viruses were picked and expanded by infecting the 293 cells. To screen for potential recombinants, viral DNA was purified from crude plate lysates using the QIAamp Blood kit as suggested by the manufacturer (Qiagen, Santa Clarita, CA). PCR was performed using several primer pairs specific for the adenovirus E1 sequence that spanned the desired AFP inserts, and the PCR products were digested with restriction endonucleases to confirm the structure.

CV840, derived from CP686 and pBHG10 transfection, and CV732, derived from CP219 and pBHG10 transfection, were also generated in this study for the comparison with CV890. CV732 was designed to be substantially equivalent to AvE1ao4i containing a single AFP driving E1A in an $E3^-$ adenovirus as described previously (15). CV730, an E1A-deleted adenovirus mutant;[3] CV702, an E3 mutant; and CV802, a wt virus, were used as control in this study. All of the viruses were plaque purified, and structures were verified before additional characterization.

Virus Yield and One-Step Growth Curves. Six-well dishes (Falcon) were seeded with 5×10^5 cells/well for 24 h before infection. Cells were infected at a MOI of 2 pfu/cell for 3 h in serum-free medium. After 3 h, the virus-containing medium was removed, monolayers were washed three times with PBS, and 4 ml of complete medium (RPMI 1640 with 10% fetal bovine serum) was added to each well. After infection (72 h), cells were scraped into the culture medium and lysed by three cycles of freeze-thaw. The one-step growth-curve time points were the time when samples were harvested after infection. Two independent infections of each virus-cell combination were titered in duplicate on 293 cells (10).

Northern Blot Analysis. Hep3B or HBL100 cells were infected at an MOI of 20 pfu/cell with either CV802 or CV890 and harvested 24 h after infection. Total cellular RNA was purified using the RNeasy protocol (Qiagen). The Northern blot was conducted using NorthernMax Plus reagents (Ambion, Austin, TX). RNA (5 μg) was fractionated on a 1% agarose, formaldehyde-based denaturing gel and transferred to a BrightStar-Plus (Ambion) positively charged membrane by capillary transfer. The antisense RNA probes for E1A (adenovirus genome 501 bp-1141 bp) or E1B (1540 bp-3910 bp) were PCR products cloned in pGEM-T easy (Promega) and transcription labeled with [α^{32}P] UTP. Blots were hybridized at 68°C for 14 h with ZipHyb solution and washed using standard methods (Ambion). Membranes were exposed to BioMax film (Kodak).

Western Blot Analysis. Hep3B or HBL100 cells were infected at MOI of 20 pfu/cell with either CV802 or CV890 and harvested 24 h after infection. Cells were washed with cold PBS and lysed for 30 min on ice in a NP40 equivalent [50 mM Tris (pH 8.0), 150 mM NaCl, and 1% IGEPAL CA360] (Sigma Chemical Co., St. Louis, MO), 0.5% sodium deoxycholate, and protease inhibitor mixture (Roche, Palo Alto, CA). After 30 min of centrifugation at 4°C, the supernatant was harvested and the protein concentration determined with the protein assay ESL kit (Roche). Fifty μg of protein/lane were separated on 8–16% SDS-PAGE and electroblotted onto Hybond ECL membrane (Amersham Pharmacia, Piscataway, New Jersey). The membrane was blocked overnight in PBS with 0.1% Tween 20 supplemented with 5% nonfat dry milk. Primary antibody incubation was performed at room temperature for 2–3 h with PBS with 0.1% Tween 20/1% milk diluted antibody followed by wash and 1-h incubation with diluted horseradish peroxidase-conjugated secondary antibody (Santa Cruz Biotechnology Inc., Santa Cruz, CA). ECL (Amersham Pharmacia) was used for signal detection. E1A antibody (clone M58) was from NeoMarkers (Fremont, CA), E1B-21kD antibody was from Oncogene (Cambridge, MA). All of the antibodies were used according the manufacturer's instruction.

Cell Viability Assay and Statistical Analysis. To determine the cell killing effect of CV890 and doxorubicin in combination treatment, a cell viability assay was conducted as described previously with modifications (21). On 96-well plates, cells of interest were seeded at 10,000 cells/well 48 h before infection. Cells were treated with virus alone, drug alone, or in combination. Cell viability was measured at different time points by removing the medium, adding 50 μl of 1mg/ml solution of MTT (Sigma Chemical Co.), and incubating for 3 h at 37°C. After removing the MTT solution, the crystals remaining in the wells were solubilized by the addition of 50 μl of isopropanol followed by 30°C incubation for 30 min. The absorbency was determined on a microplate reader (Molecular Dynamics) at 560 nm (test wavelength) and 690 nm (reference wavelength). The percentage of surviving cells was estimated by dividing the $OD_{550} - OD_{650}$ of virus- or drug-treated cells by the $OD_{550} - OD_{650}$ of control cells. Six replica samples were taken for each time point, and each experiment was repeated at least three times.

For statistical analysis of synergy, CurveExpert (shareware by Daniel Hyams, version 1.34) was used to plot the dose-response curves for virus and drugs. Based upon the dose-response curves, the isobolograms were made according to the original theory of Steel and Peckham (22) and as modified by Aoe *et al.* (23).

Animal Studies. Six to eight-week-old athymic BALB/C *nu/nu* mice were obtained from Simonson Laboratories (Gilroy, CA) and acclimated to labora-

[3] D. R. Henderson and D-C. Yu, unpublished data.

tory conditions 1 week before tumor implantation. Xenografts were established by injecting s.c. 1×10^6 Hep3B, HepG2, or LNCaP cells suspended in 100 μl of RPMI 1640. When tumors reached between 200 and 300 mm^3, mice were randomized and dosed with 100 μl of test article via intratumoral or tail vein injection. Tumors were measured in two dimensions by external caliper, and volume was estimated by the formula [length (mm) $\times$ width $(mm)^2$]/2. Animals were humanely killed when their tumor burden became excessive. Serum was harvested weekly by retro-orbital bleed. The level of AFP in the serum was determined by AFP Immunoassay kit (Genzyme Diagnostics, San Carlos, CA). The difference in mean tumor volume and mean serum AFP concentration between treatment groups was compared for statistical significance using the unpaired, two-tailed *t* test. Immunohistochemical analysis of tumors for adenovirus replication was conducted by following a procedure described previously (9).

RESULTS

Construction of Recombinant Adenoviruses Containing AFP-controlled E1A-IRES-E1B Bicistronic Cassette. Tumor-specific TREs to control ARCA replication have been applied in CV706 and CV787 for prostate cancer therapy. In the current study, we additionally explored the application of ARCA technology in primary liver cancer. Because AFP is the only well-characterized HCC-specific biomarker available, we focused on using AFP TRE to make better transcriptionally controlled adenovirus variants. In our preliminary studies, different recombinant adenovirus variants generated by using single AFP TRE to control E1A alone (AFP-E1A), E1B alone (E1A-AFP-E1B), or dual AFP TREs to control E1A and E1B separately (AFP-E1A-AFP-E1B) were compared. Among these viruses, dual AFP control on E1A and E1B separately had higher specificity than AFP control of either the E1A or E1B alone (data not shown). However, viruses with two AFPs, AFP-E1A and AFP-E1B, are unstable because of homologous recombination. Therefore, we devised an alternate strategy to place both the *E1A* and *E1B* genes under the control of a single AFP TRE thereby constructing CV890. We compared CV890 with CV732, a virus with a single AFP TRE driving the *E1A* gene, for both *in vitro* specificity and *in vivo* efficacy. We went on to demonstrate synergy of CV890 and doxorubicin both *in vitro* and *in vivo* resulting in a treatment protocol that could eliminate large, preexistent HCC tumors with a single treatment of CV890.

To control both *E1A* and *E1B* genes with single AFP, an EMCV IRES structure was applied to build an artificial E1A-IRES-E1B bicistronic expression cassette. EMCV IRES has been well characterized and applied for mediating secondary gene expression (24). This artificial E1A-IRES-E1B bicistronic cassette enables both E1A and E1B to form a single unit for transcription, whereas the IRES structure gives the internal translation initiation for E1B translation. In the current study, E1A-IRES-E1B bicistronic cassette was placed under the transcriptional control of the AFP TRE to target the new ARCAs to AFP-producing cells. Fig. 1 illustrates the schematic structure of resultant viruses CV890 and CV840 that have intact E3 or deleted E3, respectively. CV702 and CV802 have wt E1 region and are used as wt Ad5 controls with or without E3 deletion, respectively (10). Another ARCA, CV732, containing single AFP to control only E1A expression, was used to compare with CV890 and CV840. CV787, a prostate cancer-specific adenovirus variant (9), was used as a negative control for *in vivo* liver cancer xenograft animal studies. CV730 was an E1A-deleted mutant and was also used as a control in the current study.

***In Vitro* Specificity Comparison of Viruses with AFP-controlled E1A Alone or E1A and E1B Together.** Previously, we have demonstrated that double TREs controlling E1A and E1B separately can lead to better specificity than just one TRE controlling E1A (9). In the current study, we additionally tested this observation to improve the

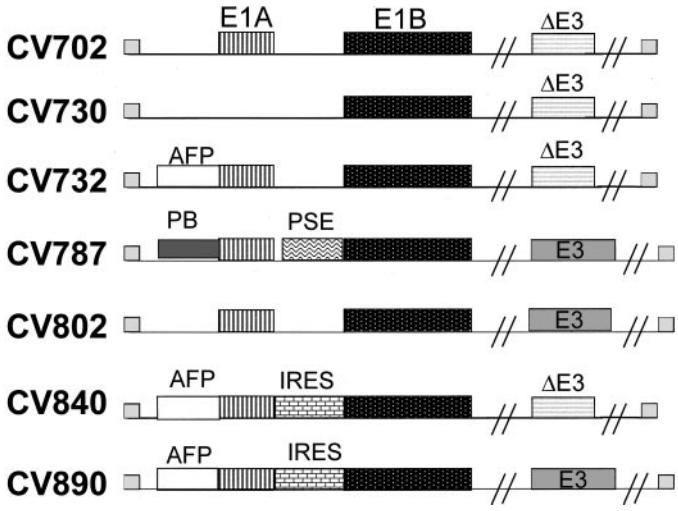

Fig. 1. Schematic DNA structures of different ARCAs (not to scale). CV802 and CV702 are the wt Ad5 with intact or deleted E3, respectively. CV730 is an E1A-deleted mutant without E3. CV787 is a prostate cancer-specific ARCA, and the other viruses are liver cancer-specific ARCAs. Liver cancer-specific viruses contain transcriptional regulatory sequence from the *AFP* gene engineered into adenovirus genome to drive transcription of E1A (CV732), or E1A/E1B bicistronic cassette linked by the IRES structure from ECMV (CV840 and CV890). Boxes at both ends are inverted terminal repeats. Other rectangles are labeled for their function in the viral genome. *PB,* probasin promoter; *PSE,* prostate-specific enhancer.

specificity of adenovirus variants by using a single AFP controlling the E1A-IRES-E1B bicistronic cassette. To demonstrate the advantage of using the new strategy, we first compared the replication specificity profiles of CV890 ($E3^+$) and CV840 ($E3^-$) to CV732 ($E3^-$). CV732 has been characterized to be a candidate liver cancer-specific adenovirus variant in preliminary studies (results not shown) and is similar to the adenovirus described previously, AvE1a04 i, in which the AFP TRE was applied to control E1A alone (15). Fig. 2*A* shows the virus yield assay controlled by wt CV702 and CV802 in a panel of different tumor cell lines including AFP^+ cells (HepG2 and Hep3B; see below for AFP status) and AFP^- cells (Chang liver cell, UM-UC-3, SW 780, CoLo 201, and U118 MG). Our results showed that all of the CV890, CV840, and CV732 have clear cell selective patterns. Whereas wt viruses CV702 and CV802 replicate well in all of the cell lines, the AFP viruses CV732, CV840, and CV890 are attenuated by 100- 100,000-fold when compared with wt controls in AFP^- cells. From the parallel comparison of three variants, both CV890 and CV840 have a better replication specificity than CV732. In AFP^- cells, CV890 showed 100,000-fold attenuation, whereas CV732 only showed 100-fold attenuation. In addition, CV890 and CV840 showed a 5-fold increase in replication efficiency in AFP^+ cells compared with CV732. Finally, in all of the AFP^- cells, although the initial infection was at MOI of 2, the burst size for both CV890 and CV840 was 1 pfu/cell, suggesting that the virus replicates poorly. For CV732, however, there is definitely a clear replication in the AFP^- cells with an average burst size of 100 pfu/cell. This increased virus replication or leakiness is attributable to reduced transcriptional control.

Cytotoxicity of CV890 and CV732 was then compared in the MTT cell viability assay. Hep3B and Chang liver cells were infected at an MOI of 0.01 with CV732, CV802, or CV890. Data presented in Fig. 2*B* indicated that CV802 was toxic to Hep3B cells and Chang liver cells regardless of AFP status, whereas CV890 and CV732 were only toxic to AFP-producing Hep3B cells but not to AFP^- Chang liver cells. Interestingly, when both CV890 and CV732 were toxic to AFP-producing Hep3B cells, CV890 had a superior cytotoxicity. For example, there were no surviving CV890-infected Hep3B cells 9 days

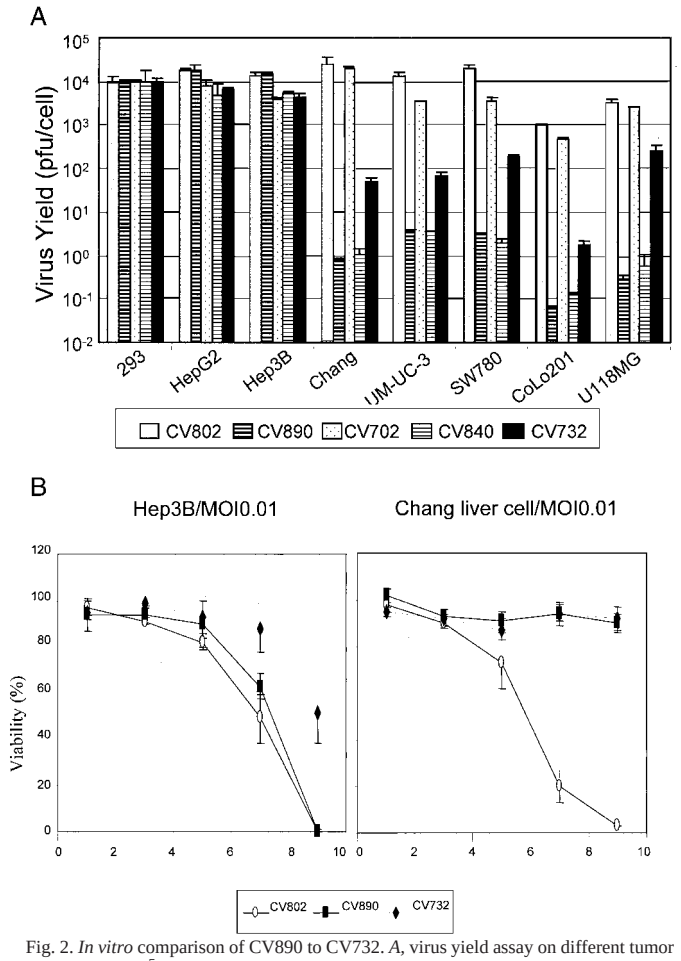

Fig. 2. *In vitro* comparison of CV890 to CV732. *A*, virus yield assay on different tumor cells. Cells (5×10^5) were infected with different viruses at MOI of 2. After 72 h of viral infection, cell lysates were harvested and titrated by plaque assay on 293 cells. The numbers from 293 cell control were used for normalization to determine virus yield on other cells. Duplicate titrations were scored for virus yield, and the means were plotted; *bars*, ± SD. *B*, cytotoxicity comparison on permissive and nonpermissive cells. Cells in the 96-well plates were infected with different viruses at MOI of 0.01. At indicated time, cell viability was determined by MTT assay based on cell controls as designated 100%. Results from 18 repeat wells were averaged; *bars*, ± SD.

after infection, whereas the viability of CV732-infected Hep3B cells was 50%. The *in vitro* comparison in Fig. 2 suggests that CV890 has a better replication specificity and killing ability to the target cells than CV732. Therefore, the strategy of using single AFP to control the E1A-IRES-E1B bicistronic cassette is better than the strategy of controlling E1A alone. On the basis of the comparison in different AFP-controlled variants, we focused additional preclinical work on CV890.

Transcription and Translation of the E1A-IRES-E1B Bicistronic Cassette of CV890 in Different Cells. In wt adenovirus infection, *E1A* and *E1B* genes produce a family of alternatively spliced products. It has been found that there are five E1A mRNAs, but among them the 12S (880 nts) and 13S (1018 nts) mRNAs are the dominant ones at both early and late times after infection. The 12S and 13S mRNAs encode the gene products of 243 amino acids (243R) and 289 amino acids (289R) respectively (25). The two major E1B transcripts are 12S (1031 nts) and 22S (2287 nts) mRNAs that encode the M_r 19,000 and M_r 55,000 E1B proteins respectively. E1B 12S mRNA only encodes the M_r 19,000 product, whereas the 22S mRNA encodes both the M_r 19,000 and M_r 55,000 products because of different initiation sites during translation. In the current study, the generation of E1A-IRES-E1B bicistronic cassette was expected to change the pattern of E1A and E1B transcripts in viral infection. Therefore, Northern blot analysis was conducted to evaluate the steady-state level of E1A and E1B transcripts. First, CV802 or CV890 was infected to Hep3B (AFP^+) or HBL100 (AFP^-) cells for 24 h. The total RNA samples were separated on agarose gels and processed for Northern blot by hybridizing to antisense RNA probes. The Northern blot with E1A probe visualized the 12S and 13S mRNAs in both Hep3B and HBL100 cells infected with CV802 (Fig. 3*A*). For CV890, E1A transcripts can only be seen in Hep3B cells but not in HBL100 cells, indicating the conditional transcription of E1A. It is of interest to find that in CV890, there is only one large transcript (about 3.5 kb marked by an *arrow* in Fig. 3*A*), whereas the 12S and 13S mRNAs are no longer present. This large transcript indicates the continuous transcription of E1A-IRES-E1B bicistronic cassette, suggesting an alteration of viral E1A splicing pattern in CV890. In the *bottom panel* of Fig. 3*A*, transcription of E1B from CV890 is also AFP-dependent. It is clear that both 12S and 22S mRNAs of E1B are present in wt CV802 samples, whereas the 12S mRNA and an enlarged 22S mRNA (3.5 kb) are present in CV890-infected Hep3B cells. The identity of this enlarged mRNA is the same 3.5-kb transcript as visualized in the E1A blot, which is from the

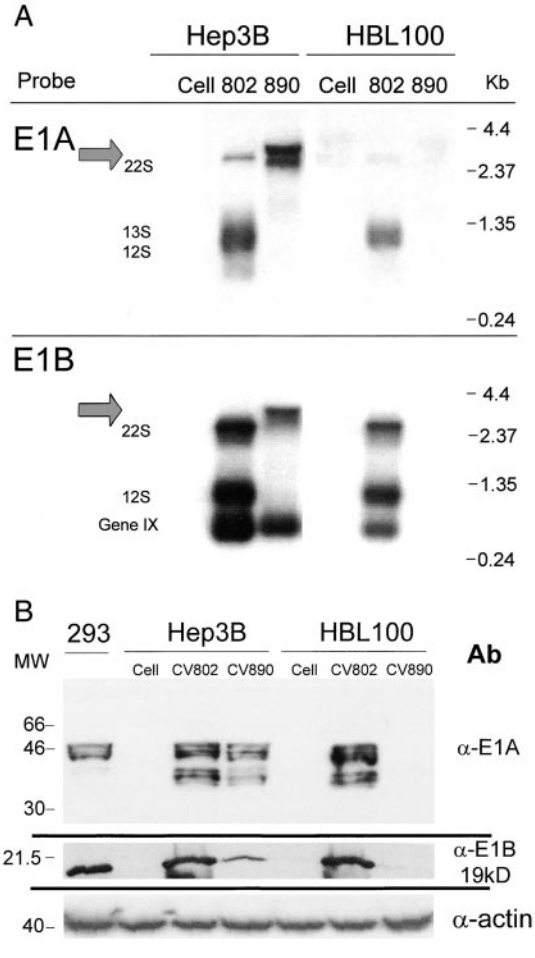

Fig. 3. Northern and Western blots of CV890 E1A-IRES-E1B expression. *A*, Northern blot of RNA prepared from CV890- or CV802-infected Hep3B and HBL100 cells 24 h after infection. Total RNA was separated on 1% agarose gel and transferred to membrane. ^{32}P-labeled antisense RNA probes were hybridized to the membrane. Membrane was processed with high stringency washing and exposed to BioMax film. Labels on *left*, probe and name of the transcript. Labels on *right*, size of RNA. *Arrows*, position of large transcript from E1A-IRES-E1B bicistronic cassette. *B*, Western blot of protein prepared from CV890- or CV802-infected Hep3B and HBL100 cells. Cell lysate (50 μg) in each lane was separated on 8–16% PAGE and blot to membrane and probed with different antibodies (*labeled on right*). After incubation with secondary antibody, image was developed by ECL.

transcription of E1A-IRES-E1B bicistronic cassette. Therefore, the E1B mRNA is tagged after E1A mRNA in this large transcript. This large transcript contains all of the coding information for E1A and E1B, M_r 19,000, and E1B, M_r 55,000. The mRNA splice pattern shown in CV802-infected Hep3B cells is not shown in CV890-infected Hep3B cells for the 12S mRNA where the E1B probe is missing. Meanwhile, in the E1B Northern blot, because of the selection of our E1B probe (1540 bp-3910 bp) and mRNA of the adenovirus gene IX (3580 bp-4070 bp), the hexon-associated protein was also detected. In CV890-infected Hep3B cells, gene IX expression is equivalent to that of CV802, whereas in CV890-infected HBL100, its expression was also completely shut down. This result also demonstrated that the AFP-controlled E1A-IRES-E1B expression is the key for late gene expression as well as viral replication.

Results of the same samples in Western blot also indicate that CV890 shows AFP-dependent expression of E1A and E1B (Fig. 3*B*). Under our experimental condition, E1A expression level of CV890 in Hep3B cells is similar to that of CV802 (Fig. 3*B*). However, when E1B M_r 19,000 protein was detected, it was found that the expression level was much lower than CV802 E1A (Fig. 3*B*). Previously, it has been addressed that IRES-mediated second gene has less expression (26). Taken together, CV890 infection in permissive Hep3B cells can produce normal amount of E1A and lesser amounts of E1B proteins capable of initiating a normal productive infection. In AFP$^-$ cells, however, this process was attenuated because of a lack of E1A and E1B gene transcription and translation. These data demonstrated that the expression of both *E1A* and *E1B* genes are under the control of AFP TRE, and the artificial E1A-IRES-E1B bicistronic cassette is functioning properly in CV890.

***In Vitro* Replication Specificity of CV890 in Tumor Cells and Primary Cells.** From *in vitro* comparison of virus yield, CV890 has a better specificity profile than CV732 (Fig. 2). To gain additional insights about using CV890 in liver cancer therapy, more tumor cell lines and primary cells were tested to characterize *in vitro* virus replication. First, all of the cells in the study were analyzed for their AFP status by AFP immune assay. On the basis of AFP produced in the cells and medium, all of the cells were divided into three groups: high (>2500 ng/10^6 cells/10 days), low (<600 ng/10^6 cells/10 days), and none (undetectable in our study; Table 1). It was confirmed that replication of CV890 in different cell lines correlates well with the AFP status of the host cell. In Fig. 4, among the group of liver cell lines, CV890 only replicates well in AFP$^+$ cells including Hep3B, HepG2, Huh7, SNU449, and PLC/PRF/5. The amount of AFP required for the promoter activity seems very low, because one of the hepatoma cell line, SNU449, a previously reported AFP$^-$ cell (27), produces very low AFP (~60 ng/10^6 cells/10 days) compared with other cells. Nevertheless, even with very low amounts of AFP, SNU449 cells can still support CV890 replication comparable or only slightly less than cells producing significantly higher levels of AFP such as HepG2. Compared with CV802, CV890 is attenuated 5,000–100,000-fold in cells that do not produce any AFP, including the hepatoma cell Sk-Hep1, the Chang liver cell, other tumor cells, and primary cells (Fig. 4). Taking the results from Figs. 2 and 4 together, CV890 has shown a good specificity profile from a broad spectrum of tumor cells. Among them, only the AFP$^+$ liver cells, regardless of AFP production level, are permissive for CV890.

Table 1 *AFP production in different tumor cells*

Cells	AFP (ng/10^6 cells/10 days)	
Hep3B	2645	High
HepG2	3140	High
HuH7	4585	High
SNU449	60	Low
PLC/PRF/5	600	Low
Chang	0	None
SK-Hep1	0	None
HBL100	0	None
PA-1	0	None
LoVo	0	None

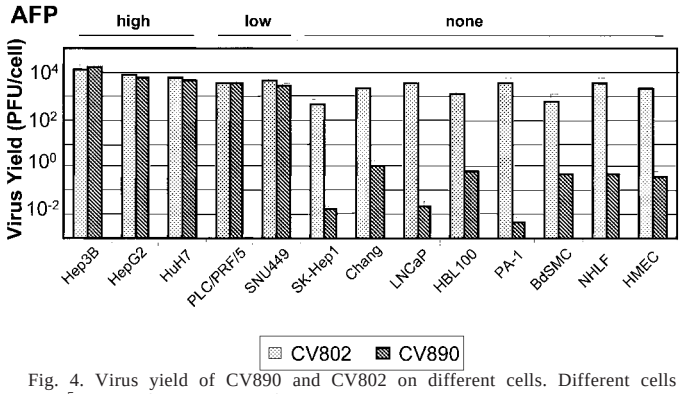

Fig. 4. Virus yield of CV890 and CV802 on different cells. Different cells (5×10^5) were infected at MOI of 2. Cell lysates were harvested at 72 h and titrated by plaque assay on 293 cells. The numbers from 293 cell control were used for normalization to determine virus yield on other cells. Duplicate titrations were scored for virus yield, and means were plotted; *bars*, ± SD. The AFP statues of different cells were grouped as high, low, and none (Table 1).

CV890 was compared with CV802 in their single step growth curves on different cells. Results presented in Fig. 5 additionally demonstrated that CV890 has similar growth kinetics to wt CV802 in AFP$^+$ cells except that virus yields are slightly lower (2–8-fold) in low AFP-producing cells. In consideration of experimental error, there is no significant difference in the replication of CV890 and CV802 in AFP$^+$ hepatoma cells. However, the growth curves of CV890 in AFP$^-$ cells showed clear attenuation. During a 5-day experiment, CV890 failed to replicate in AFP$^-$ cells including liver cell (Chang liver), ovarian cancer cell (PA-1), and primary cells (normal human lung fibroblast cells; Fig. 5). From all of the *in vitro* virus replication studies, it is clear that replication of CV890 is under the tight control of AFP TRE, and this adenovirus variant has an excellent specificity profile of preferentially targeting AFP-producing HCC cells.

***In Vivo* Specificity and Efficacy of CV890.** The specificity of CV890 was also evaluated in animals bearing prostate cancer (PSA-producing but AFP$^-$) LNCaP xenografts. In this *in vivo* test, nude mice with prostate xenografts were i.v. injected with either CV890 or CV787, a prostate cancer-specific adenovirus variant (9). Tumor volumes were documented and indicated that only CV787 had a significant antitumor efficacy in LNCaP xenografts, whereas tumors in the animals treated with CV890 grew from 400 mm^3 to ~1200 mm^3 in 6 weeks, similar to the group treated with vehicle (data not shown). This study indicates that CV890 does not attack the LNCaP xenograft and maintains the desired specificity profile under *in vivo* conditions.

To evaluate *in vivo* antitumor efficacy of CV732 (E3$^-$) and CV890 (E3$^+$), different studies were carried out in the nude mouse model harboring human hepatoma xenografts. We have shown previously that the addition of the E3 region of adenovirus significantly increased the antitumor activity of the prostate-specific adenovirus CV787 using PSA$^+$ LNCaP mouse xenografts (9). BALB/c-*nu/nu* mice with Hep3B xenografts were established. Tumor-bearing animals were challenged with single or multiple doses of CV730, CV732, and CV890 via tail vein i.v. administration. Tumor volume and serum levels of AFP were monitored weekly. Animals harboring 300 mm^3 Hep3B xenografts were grouped ($n = 7$) and injected with vehicle

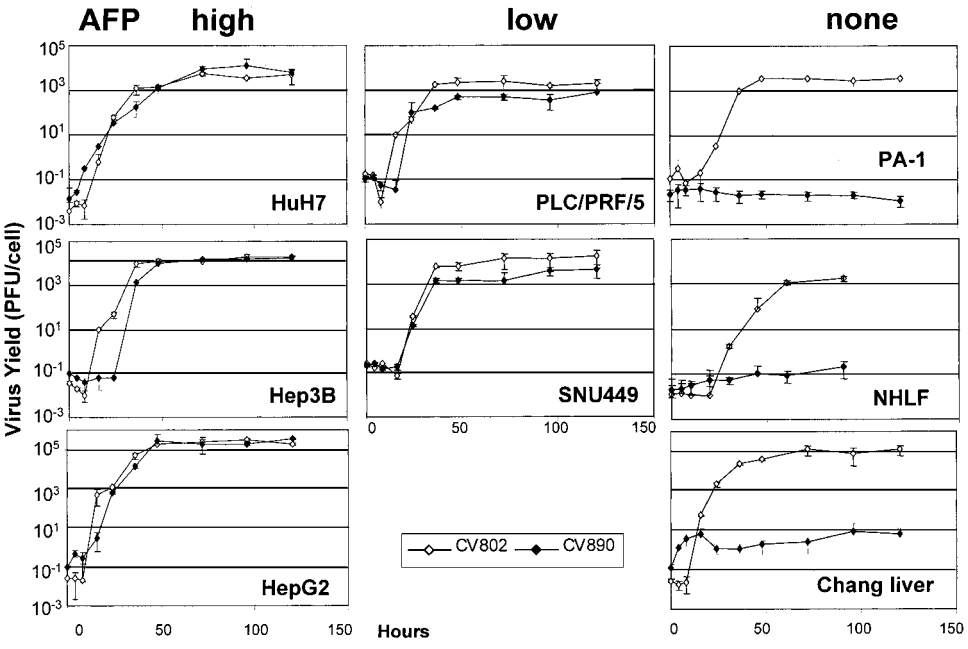

Fig. 5. Growth curves of CV890 and CV802 in different cells. Cells were infected at MOI of 2. Cell lysates were harvested at indicated times and titrated by plaque assay on 293 cells. *Error bars*, SD of mean from two different assays. AFP statues of cell were grouped as high, low, and none (Table 1). Virus yield scales are labeled on *far left panel*.

alone (control group), CV890 (1×10^{11} particles/dose), CV730 (1×10^{11} particles/dose), or CV732 (1×10^{11} particles/dose). In Fig. 6, the Hep3B xenograft was shown to be very aggressive, and tumors grew 10-fold in 5 weeks. No difference in tumor volume was observed between vehicle group and CV730 group (data not shown). In contrast, a single i.v. administration of CV890 showed significant tumor growth inhibition. In the CV732 group, single-dose i.v. injection also reduced the tumor growth as compared with the control group; however, CV732 was much less effective compared with CV890. For example, the average tumor volume of the CV890-treated group remained unchanged or slightly decreased in the course of the 6-week study, whereas tumors treated with CV732 increased from 274 mm^3 (relative tumor volume of 100%) to 1038 mm^3 (relative tumor volume 544%). Both the control group and CV732 group were terminated at week 6 because of excessive tumor size. Previously, CV732 has been demonstrated that it could restrict the hepatoma tumor from growth after 5 doses of i.v. administration (data not shown). Similar efficacy can be achieved with just a single i.v. administration of CV890, indicating that under *in vivo* condition, CV890 has better efficacy than CV732 to hepatoma xenografts. In this experiment, it was of interest that three of seven CV890 treated mice were tumor-free 3 weeks after treatment. However, in the CV732 group, xenografts in two mice stopped growing, but none of treated animals were tumor-free through the 6-week experiment. There was no tumor reduction in this group or the control group of animals. By statistical analysis, the differences in mean relative tumor volumes and serum AFP concentrations between CV890-treated and CV732-treated or vehicle-treated tumors are significant ($P < 0.01$; results not shown). Taken together, these studies show that CV890 has a significant antitumor activity, and its oncolytic efficacy is significantly better than CV732, an adenovirus variant similar to AvE1a04 I, in which a single AFP TRE was used to drive the *E1A* gene (15). As described previously and shown clearly in Fig. 1*A* comparing CV840 and CV890, the increased antitumor activity of CV890 compared with CV732 and AvE1a04 i can be attributed to the addition of the E3 region of adenovirus (9).

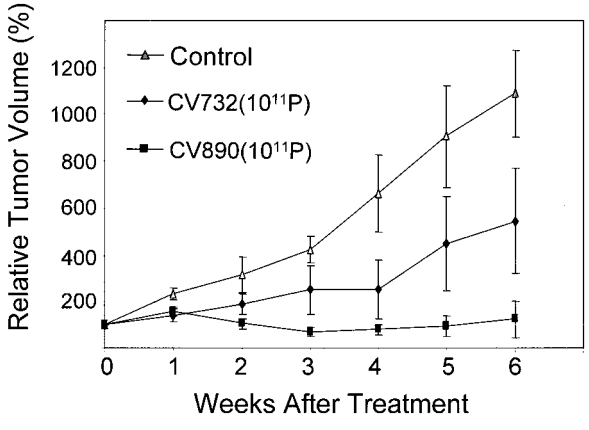

Fig. 6. *In vivo* efficacy comparison of CV890 and CV732. The nude mice with preplanted Hep3B tumors were grouped ($n = 6$) and injected with CV890 or CV732 (1×10^{11} particles/dose) or vehicle in the control group [50 mM Tris (pH 8.0)/1 mM $MgCl_2$/10% glycerol]. Tumor size was measured weekly, and tumor volume was normalized as 100% at day of treatment. *Error bars*, SE (SD/square root of group number).

Virus replication within Hep3B tumors was documented by immunohistochemical staining of tumor sections using polyclonal antibodies to Ad5 (9). Tumor section was collected from animals 7 days after treatment with different viruses. No evidence of virus replication was found in the tumors treated with either vehicle or CV730, whereas positively stained cells were viable in 10% of the CV890-treated tumors; infected cells were predominantly located near the tumor vasculature (data not shown).

Synergistic Antitumor Efficacy of CV890 in Combination with Chemotherapeutic Agents. Previously, we have demonstrated *in vitro* and *in vivo* that the combination of CV787 with paclitaxel or docetaxel leads to synergistic antitumor (20). In the current study, different chemotherapeutic agents were tested in combination with CV890 for their *in vitro* cell killing effect in Hep3B cells. We optimized drug concentration to a certain extent that it would not generate extensive cytotoxic effect by itself. Under such conditions, some agents had shown higher cell killing effect in combination with CV890. Among them, doxorubicin, a drug currently used in the treatment of HCC (6), showed synergistic cytotoxicity with CV890. Fig. 7*A* is an example of using doxorubicin together with CV890 on Hep3B cells. Doxorubicin at 10 ng/ml did not generate cytotoxicity, whereas CV890 at an MOI of 0.01 (pfu/cell) destroyed 35% of the cells by day 9. However, when both doxorubicin and CV890 were

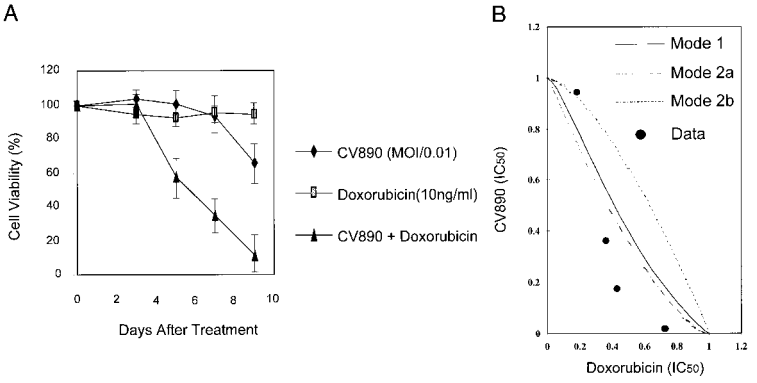

Fig. 7. *In vitro* synergistic effect of CV890 with doxorubicin. *A*, cell viability measured by MTT at different times. Hep3B cells were treated with CV890 at MOI of 0.01 or doxorubicin at 10 ng/ml or CV890 (MOI of 0.01) and doxorubicin (10 ng/ml) together. Cell viability was normalized as 100% at treatment start (day 0). Cell viability was determined by comparing the $OD_{550} - OD_{650}$ of treated cells to the $OD_{550} - OD_{650}$ of mock infected wells. *Error bars*, SD of mean from repeated samples. *B*, isobologram analysis of observed data. Concentration that produced 50% cell growth inhibition is expressed as 1 in the ordinate and abscissa of the isobologram with defined line of modes I, IIa, and IIb from the method by Steel and Peckham (22). Data points for the combination fell within the envelope of additivity or were smaller than that of the predicted minimum data, indicating that sequential exposure to the two agents produced an synergistic effect.

applied together, 90% of the cells were killed 9 days after treatment. To determine the potential synergistic effect from the combination treatment, the MTT cell viability data were subjected to additional statistical analysis. Fig. 7*B* shows a representative 50% cell growth inhibition isobologram of doxorubicin and CV890 on Hep3B cells at day 5. First, the dose-response curves of doxorubicin alone or CV890 alone were made (result not shown). On the basis of the original theory of Steel and Peckham (22) and method by Aoe *et al.* (23), three isoeffect curves (modes I, IIa, and IIb) were constructed. A combination that gives data points to the left of the envelope of mode IIb line can be described as supra-additive (synergism; Ref. 20). From this isobologram, several data points were in the synergy area, indicating that the combination of CV890 and doxorubicin provides synergistic effects on the killing of Hep3B cells.

Although CV890 alone has good antitumor activity, we applied combination therapy with doxorubicin for *in vivo* evaluation of synergy. Animals harboring 300-mm^3 Hep3B xenografts were grouped ($n = 6$) and injected with vehicle alone (control group), CV890 alone (1×10^{11} particles/dose), doxorubicin alone (10mg/kg), or CV890 in combination with doxorubicin. Fig. 8 shows weekly changes in the relative tumor size normalized to 100% at day 1. In this experiment, by week 6, animals in the control group experienced tumor growth of 700% of baseline, whereas in the CV890 group and the combination group, animals experienced tumor reduction or were tumor-free. Of the eight Hep3B xenografts treated with CV890 alone, three animals (37.5%) had no palpable tumor at week 5, and another three animals experienced tumor regression of >60%. In the combination group, four of eight animals were tumor-free from week 5, and the other four animals experienced a tumor reduction of 95%. All of the animals in the CV890 and combination groups were alive, and the tumor was suppressed even 10 weeks after treatment, whereas the control animals were sacrificed for excessive tumor burden after week 6 (result not shown). CV890 also caused a drop in the serum AFP concentration in these mice (data not shown). Statistical analysis shows that differences in mean relative tumor volumes and serum AFP concentrations between CV890 and vehicle-treated group or combination and doxorubicin-treated group are significant at different times ($P < 0.005$; results not shown). The strong efficacy in the combination treatment shows that a single i.v. injection of CV890 in combination with doxorubicin can eradicate aggressive Hep3B xenografts in most animals.

DISCUSSION

Recently, oncolytic viruses have become an active area in cancer gene therapy (28). We have initiated clinical trails with transcriptionally regulated tumor-specific adenovirus variants, CV706 and CV787, for prostate cancer. In the current study, we extended our ARCA technology to primary liver cancer by the construction and characterization of CV890.

In the ARCA technology, the TREs placed to control E1A or E1B are the switches to turn on adenovirus replication. After adenovirus penetration, only the cells that provide the requisite transcription factors to turn on the TRE switches will support productive viral replication. In the current study, this rational was additionally verified in CV890, an adenovirus variant created with a new strategy. To control both *E1A* and *E1B* genes with single AFP TRE, we constructed an E1A-IRES-E1B bicistronic cassette by replacing the E1A-E1B junction sequence with the ECMV IRES fragment. This bicistronic cassette was placed under the control of an AFP TRE generating CV890. Transcription of both *E1A* and *E1B* genes of CV890 was found to be under the tight control of AFP TRE and translation of the E1B mediated by EMCV-IRES, as designed. Transcription of the E1A-IRES-E1B bicistronic cassette forms an enlarged 22S mRNA that has all of the coding genes for E1A and E1B. When this cassette was driven by the AFP TRE, E1 transcripts were only found in AFP^+ cells (Fig. 3*A*). E1A and E1B proteins were detected only in the CV890-infected Hep3B cells (AFP^+) but not in AFP^- HBL-100 cells (Fig. 3*B*). These data demonstrated that both the E1A-IRES-E1B transcription and translation in CV890 are AFP-dependent. This is the first effort to alter the adenovirus E1 transcription pattern to control both E1A and E1B expression by a single tumor-specific TRE.

We also found the resulting virus, CV890, has a better specificity and efficacy profile than CV732, a replicating adenovirus containing a single AFP TRE driving E1A in an $E3^-$ virus background. CV732 was designed to be functionally identical to AvE1a04 I as described previously (15).

For specificity, we compared CV890 with CV732 *in vitro* in various cell lines. Preliminary studies demonstrated that the *E1A* gene of CV732 is tightly controlled by the AFP TRE, and the *E1B* gene is driven by the endogenous adenovirus E1B promoter (data not shown). Burst size data showed that CV732 produced 100–1,000 fewer infectious virus particles in AFP^- cells as compared with AFP^+ cells. Burst size data also showed that CV890 actually had a higher replication efficiency (2–5 times higher) in AFP^+ cells than CV732. In contrast, in AFP^- cells, CV890 gave additional 100-fold attenuation when compared with CV732 (Fig. 2*A*). The overall replication difference between AFP^+ and AFP^- cells were 100-1000 fold for CV732 and 5,000–100,000-fold for CV890, demonstrating the marked improvement in replication selectivity of CV890 over CV732. Thus, the AFP TRE controlling the E1A-IRES-E1B bicistronic cassette clearly leads to a better restriction of virus replication to AFP-producing cells than a single AFP TRE driving E1A alone. For cytotoxicity comparison between CV890 and CV732, we conducted virus-killing kinetics

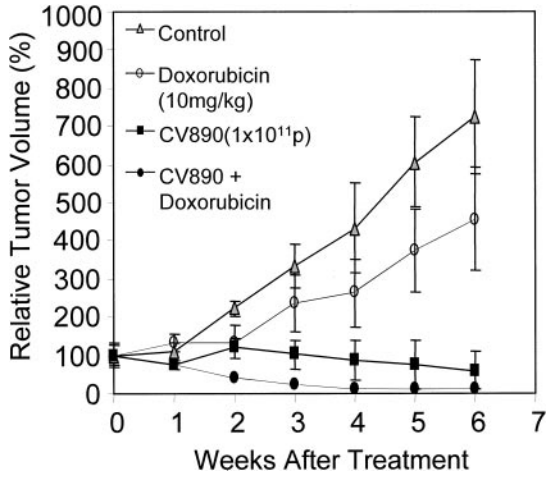

Fig. 8. *In vivo* efficacy of CV890 and doxorubicin combination treatment. Hep3B nude mouse xenografts were grouped ($n = 8$) and treated with CV890 alone (1×10^{11} particles/dose, i.v.), doxorubicin alone (10 mg/kg, i.p.), CV890 and doxorubicin combination (1×10^{11} particles of CV890 through tail vein and 10 mg/kg doxorubicin, i.p.), or vehicle control. Tumor size was measured weekly, and tumor volume was normalized as 100% at day of treatment. *Error bars*, SE. Student *t* test between each group showed difference ($P < 0.05$ between CV890 and CV890/doxorubicin combination treatment group).

on Hep3B (AFP^+) and the control Chang liver cells (AFP^-). The MTT assay demonstrated that CV890 has a significantly better cytotoxicity on the target Hep3B cells than CV732 (Fig. 2*B*).

To evaluate cancer drugs, therapeutic index is a ratio of the doses at which therapeutic effect and toxicity occur. Both virus burst size assay and growth curve assay data indicated that, at a given dose of CV890, target AFP^+ cells can produce 5,000–100,000 more viruses than nontarget AFP^- cells, demonstrating an *in vitro* therapeutic index of 5,000–100,000 to 1. The high specificity of CV890 likes is not achievable by other types therapy. For example, chemotherapeutics, such as alkylating agents and DNA synthesis inhibitors, target both malignant and normal cells, resulting in therapeutic indices of 2:1 to 6:1 (29). However, as shown in Table 1 and Fig. 4, even low levels of expression of AFP (60 ng/10^6 cells/10 days) can lead to activation of the AFP TRE within CV890 and support replication of adenovirus. Indeed, a 75-fold difference in AFP levels in different cells only slightly reduced virus yield. This point has significant implications in restricting the TREs suitable for the design of replicating oncolytic adenoviruses to treat cancer. Namely, proposed tumor markers that are "enriched" in or "overexpressed" in tumor cells may not offer a TRE with sufficiently tight regulation to yield the desired specificity. Rather, TREs that are expressed "only" in the target tumor cells or in medically unimportant tissues from a clinical side-effect profile may be suitable.

CV890 also showed much better antitumor efficacy than CV732 in the human liver cancer Hep3B mouse xenograft model (Fig. 6). Tumor reduction was achieved in all of the animals after receiving a single i.v. administration of CV890, whereas CV732 could only slow down or stop the tumor growth in a low percentage of animals, but had no tumor reduction during the entire course of the experiment. In most animals that received a single dose of CV732 via tail vein i.v. administration, tumors kept growing and caused animal death from excessive tumor burden after 6 weeks. Similar animal results have been reported in an AvE1a04 i study that showed 20–50% of animal loss after 7–13 weeks (15). In another study, AFP-controlled E1A was used to generate a pair of complementary adenoviral vectors for HuH7 xenograft treatment (19). After 3 weeks, HuH7 tumor growth was inhibited by intratumoral injection. However, there was no clear tumor reduction, and the dual vector system was concluded to have less oncolytic potency (19). Taken together, our *in vitro* and *in vivo* results presented in the current study demonstrated that CV890 not only has a significantly higher specificity (100-fold better), but also exhibits much better antitumor efficacy than adenovirus variants including CV732 and AvE1a04 i. This increased efficacy is attributable to the reincorporation of the adenovirus E3 region as described previously (9).

Current treatment for primary liver cancer often fails when the cancer has developed multiple foci or spread beyond the liver (3–5). Our data suggest that virotherapy with CV890 may provide a potential good treatment for AFP-producing HCC. Previous work has demonstrated that it is possible to achieve a high transduction efficiency of hepatocytes by i.v. administration of adenovirus (30–32). Because the majority of liver tumors derive their blood supply from the hepatic artery, whereas normal liver is fed by the portal vein, it might be possible to direct the virus to the tumor tissue by injecting it into the hepatic artery. Furthermore, the replicating virus-infected cells produce progeny that can infect and kill neighboring target cells. This is a significant advantage over nonreplicating vectors of which the utility has been limited thus far by inefficient tumor cell transduction. This was supported by our animal study that i.v.-administered CV890 was able to cause tumor regression or eradication in 90% of the treated animals without toxicity (Fig. 8), and extensive virus-infected cells were observed within the CV890-treated Hep3B xenografts.

To support clinical development, we also explored the possibility of adjuvant therapy by combining CV890 with chemotherapeutic agents. A synergistic decrease of cell viability of AFP-producing cells (HepG2 and Hep3B) was observed when CV890 was combined with doxorubicin. Hep3B cells cultured with doxorubicin for 24 h before or after infection with CV890 had significantly decreased viability compared with cells treated with either agent alone. Hep3B cells treated with doxorubicin exhibited a greater burst size of CV890, whereas cytolytic selectivity of CV890 was fully remained. A synergistic antitumor efficacy of combination therapy with CV890 and doxorubicin was also observed *in vivo* in Hep3B xenografts. Tumor growth was inhibited by a single i.v. administration of CV890 at a dose of 1×10^{11} particles, whereas combination treatment of CV890 with doxorubicin eliminated tumors within 6 weeks. Statistical analysis of the *in vivo* studies indicated that the CV890 and doxorubicin combination group showed a significant synergy with a 5.3-fold higher inhibition of tumor growth over additive effect (data not shown). Our previous study with CV787, a prostate cancer-specific adenovirus variant (9, 20), and this current study demonstrate that tumor-specific viruses together with chemotherapeutic agents provide synergistic antitumor effects. Therefore, CV890 in combination with doxorubicin has strong preclinical support for clinical development.

In summary, we have successfully extended our technology platform by creating CV890, a tumor-specific adenovirus by linking two essential viral genes, *E1A* and *E1B*, with an IRES. Use of an AFP TRE-E1A-IRES-E1B cassette yields a virus of very high specificity for target cells (5,000–100,000:1) with only a single tumor-specific TRE. We also show that CV890 replication in AFP+ cells is independent of AFP production levels between 60 ng and 4500 ng AFP/10^6 cells/10 days. The TRE-E1A-IRES-E1B bicistronic cassette strategy saves space within the virus genome allowing the reincorporation of the adenovirus E3 region adding much needed antitumor efficacy. A single dose of CV890 via i.v. administration inhibits tumor growth of the very aggressive human Hep3B xenograft in BALB/c-*nu/nu* mice. Synergistic antitumor efficacy was observed both *in vitro* and *in vivo* when CV890 was combined with a chemotherapeutic agent, doxorubicin, while retaining the same specificity of destroying AFP^+ cells and leaving AFP^- cells intact. A single i.v. administration of CV890 in combination with doxorubicin eliminated distant tumors

within 4 weeks after treatment. These results support the clinical development of CV890 as an antineoplastic agent for the treatment of localized or metastatic HCC tumors.

ACKNOWLEDGMENTS

We thank Andrew Little for help in the early stages of this work; Jake Lee, Yiwei Zhang, Joseph Oh, and Jeanette Dilly for technical help; John Radzyminski, Rukmini Pennathus-Das, and Dominic Brignetti for virus production; and Drs. W. K. Joklik and Albert Owens for thoughtful discussions.

REFERENCES

1. Anonymous World Health Report 2000. Geneva: WHO, 2000.
2. Parkin, D. M., and Muir, C. S. Cancer Incidence in Five Continents. Comparability and Quality of Data. IARC Sci. Publ., *120:* 45–173, 1992.
3. Venook, A. P. Treatment of hepatocellular carcinoma: too many options? J. Clin. Oncol., *12:* 1323–1334, 1994.
4. Levin, B., and Amos, C. Therapy of unresectable hepatocellular carcinoma. N. Engl. J. Med., *332:* 1294–1296, 1995.
5. Farmer, D. G., Shaked, A., Colonna, J. O., Olthoff, K. M., Jurim, O., Colquhoun, S., Millis, J. M., and Busuttil, R. W. Radical resection combined with liver transplantation for foregut tumors. Am. Surg., *59:* 806–812, 1993.
6. Bismuth, H., Morino, M., Sherlock, D., Castaing, D., Miglietta, C., Cauquil, P., and Roche, A. Primary treatment of hepatocellular carcinoma by arterial chemoembolization. Am. J. Surg., *163:* 387–394, 1992.
7. Huang, C. C., Wu, M. C., Xu, G. W., Li, D. Z., Cheng, H., Tu, Z. X., Jiang, H. Q., and Gu, J. R. Overexpression of the *MDR1* gene and P-glycoprotein in human hepatocellular carcinoma. J. Natl. Cancer Inst., *84:* 262–264, 1992.
8. Rodriguez, R., Schuur, E. R., Lim, H. Y., Henderson, G. A., Simons, J. W., and Henderson, D. R. Prostate attenuated replication competent adenovirus (ARCA) CN706: a selective cytotoxic for prostate-specific antigen-positive prostate cancer cells. Cancer Res., *57:* 2559–2563, 1997.
9. Yu, D. C., Chen, Y., Seng, M., Dilley, J., and Henderson, D. R. The addition of adenovirus type 5 region E3 enables calydon virus 787 to eliminate distant prostate tumor xenografts. Cancer Res., *59:* 4200–4203, 1999.
10. Yu, D. C., Sakamoto, G. T., and Henderson, D. R. Identification of the transcriptional regulatory sequences of human kallikrein 2 and their use in the construction of calydon virus 764, an attenuated replication competent adenovirus for prostate cancer therapy. Cancer Res., *59:* 1498–1504, 1999.
11. Peng, S. Y., Lai, P. L., Chu, J. S., Lee, P. H., Tsung, P. T., Chen, D. S., and Hsu, H. C. Expression and hypomethylation of α-fetoprotein gene in unicentric and multicentric human hepatocellular carcinomas. Hepatology, *17:* 35–41, 1993.
12. Chen, H., Egan, J. O., and Chiu, J. F. Regulation and activities of α-fetoprotein. Crit. Rev. Eukaryot. Gene Expr., *7:* 11–41, 1997.
13. Nakabayashi, H., Hashimoto, T., Miyao, Y., Tjong, K. K., Chan, J., and Tamaoki, T. A position-dependent silencer plays a major role in repressing α-fetoprotein expression in human hepatoma. Mol. Cell. Biol., *11:* 5885–5893, 1991.
14. Watanabe, K., Saito, A., and Tamaoki, T. Cell-specific enhancer activity in a far upstream region of the human α-fetoprotein gene. J. Biol. Chem., *262:* 4812–4818, 1987.
15. Hallenbeck, P. L., Chang, Y. N., Hay, C., Golightly, D., Stewart, D., Lin, J., Phipps, S., and Chiang, Y. L. A novel tumor-specific replication-restricted adenoviral vector for gene therapy of hepatocellular carcinoma. Hum. Gene Ther., *10:* 1721–1733, 1999.
16. Berk, A. J. Adenovirus promoters and E1A transactivation. Annu. Rev. Genet., *20:* 45–79, 1986.
17. Babiss, L. E., and Ginsberg, H. S. Adenovirus type 5 early region 1b gene product is required for efficient shutoff of host protein synthesis. J. Virol., *50:* 202–212, 1984.
18. Hitt, M. M., and Graham, F. L. Adenovirus E1A under the control of heterologous promoters: wide variation in E1A expression levels has little effect on virus replication. Virology, *179:* 667–678, 1990.
19. Alemany, R., Balague, C., and Curiel, D. T. Replicative adenoviruses for cancer therapy. Nat. Biotechnol., *18:* 723–727, 2000.
20. Yu, D. C., Chen, Y., Dilley, J., Embry, M., Zhang, H., Nguyen, N., Amin, P., Oh, J., and Henderson, D. R. Antitumor synergy of CV787, a prostate cancer-specific adenovirus, and paclitaxel and docetaxel. Cancer Res., *61:* 517–525, 2001.
21. Denizot, F., and Lang, R. Rapid colorimetric assay for cell growth and survival. Modifications to the tetrazolium dye procedure giving improved sensitivity and reliability. J. Immunol. Methods, *89:* 271–277, 1986.
22. Steel, G. G., and Peckham, M. J. Exploitable mechanisms in combined radiotherapy-chemotherapy: the concept of additivity. Int. J. Radiat. Oncol. Biol. Physiol., *5:* 85–91, 1993.
23. Aoe, K., Kiura, K., Ueoka, H., Tabata, M., Matsumura, T., Chikamor, I. M., Matsushita, A., Kohara, H., and Harada, M. Effect of docetaxel with cisplatin or vinorelbine on lung cancer cell lines. Anticancer Res., *19:* 291–299, 1999.
24. Jackson, R. J., and Kaminski, A. Internal initiation of translation in eukaryotes: the picornavirus paradigm and beyond. RNA (NY), *1:* 985–1000, 1995.
25. Flint, J., and Shenk, T. Viral transactivating proteins. Annu. Rev. Genet., *31:* 177–212, 1997.
26. Mizuguchi, H., Xu, Z., Ishii-Watabe, A., Uchida, E., and Hayakawa, T. IRES-dependent second gene expression is significantly lower than cap-dependent first gene expression in a bicistronic vector. Mol. Ther., *1:* 376–382, 2000.
27. Park, J. G., Lee, J. H., Kang, M. S., Park, K. J., Jeon, Y. M., Lee, H. J., Kwon, H. S., Park, H. S., Yeo, K. S., Lee, K. U., *et al.* Characterization of cell lines established from human hepatocellular carcinoma. Int. J. Cancer, *62:* 276–282, 1995.
28. Gomez-Navarro, J., Curiel, D. T., and Douglas, J. T. Gene therapy for cancer. Eur. J. Cancer, *35:* 867–885, 1999.
29. Elliott, B. M., Jackh, R., and Jung, R. Evaluation of the genotoxicity of 4-diethylamino-4′-nitroazobenzene and seven analogues. Mutagenesis, *9:* 517–521, 1994.
30. Worgall, S., Wolff, G., Falck-Pedersen, E., and Crystal, R. G. Innate immune mechanisms dominate elimination of adenoviral vectors following *in vivo* administration. Hum. Gene Ther., *8:* 37–44, 1997.
31. Futagawa, Y., Okamoto, T., Ohashi, T., and Eto, Y. Efficiency of adenovirus-mediated gene transfer into hepatocytes by liver asanguineous perfusion method. Res. Exp. Med., *199:* 263–274, 2000.
32. Chen, Y., Yu, D. C., Charlton, D., and Henderson, D. R. Pre-existent adenovirus antibody inhibits systemic toxicity and antitumor activity of CN706 in the nude mouse LNCaP xenograft model: implications and proposals for human therapy. Hum. Gene Ther., *11:* 1553–1567, 2000.